Research Article Wiley Online Library ELECTROANALYSIS

doi.org/10.1002/elan.202100693

Synthesis, Electrochemistry, Spectroelectrochemistry, and Electrochromism of Metallophthalocyanines Substituted with Four (2,4,5-Trimethylphenyl)ethynyl Groups

Sevgi Özcan,[a] Rabia Zeynep Kobak,[a] Özlem Budak,[b] Atıf Koca,[b] and Zehra Altuntaş Bayır*[a]

Abstract: The synthesis of the novel phthalonitrile containing (2,4,5-trimethylphenyl)ethynyl moieties was performed using the palladium-catalyzed Sonogashira cross-linking methodology. Cobalt phthalocyanine was obtained with the cyclotetramerization reaction of this dinitrile derivative, while the synthesis of zinc and manganese phthalocyanines was reported by the Sonogashira coupling reaction of the appropriate iodo phthalocyanines. Voltammetric and electrochromic analyses were applied to determine the possible applications of these complexes in different electrochemical/display technologies. The rich redox responses of the complexes had a good influence on the spectroelectrochemical characters of them. Electrochromic measurements of the complexes indicated fast, and reversible color changes with reasonable optical contrasts.

Keywords: Electrochemistry · Electrochromism · Metallophthalocyanine · Sonogashira cross-coupling reaction · Spectroelectrochemistry

1 Introduction

Since the accidental discovery that led to the great revelation of phthalocyanines, these extraordinary compounds have been performing significant roles as in many research fields. Phthalocyanines (Pcs), which are tetrapyrrolic macrocyclic compounds, bear extraordinary physical and chemical properties. Thanks to the 18 π-electron delocalization in their structure, they are resilient to chemical, thermal and architectural changes [1–3]. Their stability and these wonderful features makes the contribution of Pc related compounds quite valuable in the next generation modern electronic devices, such as in electrochromic [4] and electro-luminescent displays [5], nonlinear optics [6], chemical sensors [7] and photosensitizers for photodynamic cancer therapy (PDT) of tumors [8,9]. In view of that, currently, extensive research has been going on related to the synthesis and characterization of Pc and its derived compounds in the field of electronic devices.

Phthalocyanines, being porphyrin-based macrocycles, are capable of integrating with multiple substituents, thus generating a variety of new derivatives. The substituents can be located peripherally to tetraazaisoindole macrocycle along with a metal ion coordinating with the nitrogen atoms present in the central cavity. Moreover, axial ligands can also be incorporated in the Pc core generating fifth and sixth coordination for metal ions [10–12]. All these alterations reduce π-π interactions between Pc rings and increase the distance between them. As a result, the non-aggregated substituted metal phthalocyanines have higher solubility in common organic solvents compared to the substituted phthalocyanines. Additionally, these structural changes help regulate the photophysical features of the novel Pcs [13,14].

Electrochromism is a mechanism where a material undergoes various reduction or oxidation states under electrode potential and gives a reversible color change with every redox state. Such electrochromic materials have found useful applications in display-related fields [15]. During the course of last few decades, many researchers have strived to engineer novel materials bearing extraordinary displaying technological features. Until now, the participants of the conducted researches utilized for electrochromism testing in different compounds included a number of inorganic and organic entities [16–19].

Among all the tested compounds so far, MPcs gave the best results and are excellent for fabrication of electrochromic materials. A range of colors can be obtained when these macrocycles are executed in an electrochromic device when paired alongside different substituents [4,20,21]. The groups substituted peripherally on their benzene rings can also help overcome the low solubility problem of MPcs in common organic solvents. The MPc films prepared for electrochromic devices via spin-coating method requires a high solubility in organic

[a] S. Özcan, R. Z. Kobak, Z. A. Bayır
Department of Chemistry, Science&Letters Faculty, Istanbul Technical University, Istanbul, Turkey
E-mail: bayir@itu.edu.tr
[b] Ö. Budak, A. Koca
Department of Chemical Engineering, Engineering Faculty, Marmara University, Istanbul, Turkey

Supporting information for this article is available on the WWW under https://doi.org/10.1002/elan.202100693

solvents [22]. Furthermore, the solubility as well as aggregation issues of MPc compounds can be enhanced when substituted with appropriate bulky compounds like alkynyl chains as they tend to extend the π- conjugation [23]. Introduction of alkynyl fraction helps in enhancing the solubility as well as the optical properties of synthesized MPcs [24–26]. Alkynyl portions are known to cause red shift in Q band of the novel MPcs due to the extension they cause in π-conjugation of porphyrin rings [27–29].

In this study, metal phthalocyanines symmetrically substituted with four [(2,4,5-trimethylphenyl)ethynyl] entities were being synthesized and characterized for detection of possible electrochromic properties. The redox properties of the prepared compounds were analyzed for potential electrochromic materials. It is well documented that the peak character and peak positions of the MPcs could be tailored by altering the substituent environment of the Pc ring [30]. Electron donating and withdrawing ability of the substituents influence the peak positions in addition to the reversibility of the redox couples. Here, we have aimed to increase the conjugation of the Pc ring by substituting with trimethylphenylethynyl moieties, which can increase the electron density of the complexes. This issue might alter the redox properties of MPcs and moreover influence their usage in electrochemical technologies [31]. Voltammetric analysis is needed for the newly synthesized complexes to find where they can be used in various fields, thus redox activities of MPcs were determined with detailed electrochemical analyses. Moreover, electrochromic responses of the complexes were investigated in order to indicate their possible usage in display technologies.

2 Experimental

2.1 Chemicals and Equipment

Electronic absorption spectra were carried out at room temperature. We used Scinco SD 1000 and Shimadzu 2001 UV single-beam UV-Vis diode array spectrophotometers with 1-cm path length standard cuvettes. Fourier Transform Infrared (FT-IR) spectra were acquired on a Perkin-Elmer Spectrum One FT-IR spectrometer with a unit allowing to record data in universal attenuated total reflectance mode. Proton and carbon-13 nuclear magnetic resonance spectra (NMR) were recorded in deuteriated chloroform with a Bruker 500 MHz (for ^{1}H and 100 MHz for ^{13}C) NMR spectrometer, tetramethylsilane was used as an internal reference. Mass spectra were recorded on a Bruker Microflex MALDI-TOF MS and a Perkin-Elmer Clarus 500 GC/MS.

Literature reports provide enough detail as to the preparation of 4-iodonitrophthalonitrile (**1**) and its phthalocyanines [32–35].

2.2 Electrochemistry (EC) and *in Situ* Spectroelectrochemistry (SEC)

The same procedures were used to record all the electrochemical and spectroelectrochemical measurements [36–38]. A Gamry Reference 600 Potentiostat/Galvanostat was used for cyclic voltammetric (CV) and square wave voltammetric (SWV) techniques, in an electrochemical cell having glassy carbon (GCE) working, platinum wire counter, and Ag/AgCl reference electrodes in electrochemically pure dimethyl sulfoxide (DMSO)/tetrabutylammonium perchlorate (TBAP) electrolyte. For in situ SEC and in-situ spectrochronocoulometry (SCC), a working electrode made of platinum gauze was used in a home-made thin layer quartz cell. The same potentiostat and OceanOptics QE65000 diode array spectrophotometer were employed. Modified electrodes were prepared with the cast film and spin coating techniques. Indium tin oxide (ITO) substrate was coated with MPcs with the cast-film technique and then it was protected with Nafion (Nf), which was coated on the surface of ITO/MPc with the spin-coating technique. The modified ITO/MPc/Nf electrodes were used as the electrochromic electrode for the electrochromic measurements. The electrolyte employed was acetonitrile (AN)/TBAP.

2.3 Synthesis

2.3.1 4-[(2,4,5-Trimethylphenyl)ethynyl]phthalonitrile (2)

0.290 g (1.14 mmol) of 4-iodo phthalonitrile **1** was dissolved in 10 mL of THF-triethylamine (3:7) and to this solution were added 0.008 g (0.012 mmol) [$(Ph_3P)_2PdCl_2$], 0.001 g (0.005 mmol) of CuI, and 0.197 g (1.37 mmol) 1-ethynyl-2,4,5-trimethylbenzene. The reaction mixture was heated to and maintanied at 50 °C for 24 h under N_2. The light brown precipitate formed as the reaction progressed was then precipitated in n-hexane. The precipitated solid was removed by filtration and hot methanol was used to pre-purify the solid by repeatedly washing the material. The product obtained was purified by column chromatography (stationary phase: silica gel, 1:1 CH_2Cl_2:n-hexane mixture: mobile phase). Yield: 0.22 g (71 %), mp 185 °C. FT-IR (ν, cm^{-1}): 3067–3007 (C–H, aromatic), 2973–2865 (C–H, Aliphatic), 2228 (C≡N), 2210 (C≡C), 1593 (C=C). ^{1}H NMR ($CDCl_3$): δH, ppm 7.88 (s, 1H, Ar–H), 7.80-7.76 (m, 2H, Ar–H), 7.28 (s, 1H, Ar–H) 7.04 (s, 1H, Ar–H), 2.43(s, 3H, CH_3), 2.27(s, 3H, CH_3), 2.24 (s, 3H, CH_3).^{13}C NMR ($CDCl_3$): δ, ppm 139.24, 138.14, 135.75, 135.24, 134.22, 133.42, 133.20, 131.19, 129.91, 118.20, 116.24 (C≡N), 115.28 (C≡N), 114.84, 113.70, 96.57, 88.95, 20.04, 19.86, 19.07. MALDI-TOF MS m/z: found for $[M]^+$ 270.69 (calcd. for $[M]^+$ 270.12).

2.3.2 2,9 (10), 16 (17), 23 (24)-Tetrakis [(2,4,5-trimethylphenyl)ethynyl] Phthalocyaninatocobalt (II) (2 a)

In 1.5 mL of dry 2-dimethylaminoethanol as the solvent, 0.100 g (0.367 mmol) of compound (**2**) and 0.015 g (0.115 mmol) $CoCl_2$ were mixed in a glass tube. The tube was capped and the reaction mixture was brought to 150–160 °C and kept at this temperature for 24 hours in a nitrogen atmosphere and the substituted cobalt (II) phthalocyanine was formed. The tube of reaction was cooled to room temperature and the reaction mixture was precipitated by adding 50 mL of methanol. The green-colored solid thus formed was filtered off and washed several times with methanol and acetone. The solid obtained was dried in an oven and subjected to column chromatography in which silica gel was the stationary phase and methanol: tetrahydrofuran (3:1 v: v) was the mobile phase. The mobile phase was changed to ethyl acetate, methanol, and n-hexane in the course. The yield of synthesis was 0.0135 g (13 %). mp >300 °C. FT-IR (ν, cm^{-1}): 3064–3010 (C–H, aromatic), 2917–2861 (C–H aliphatic) 2203 (C≡C). MALDI-TOF-MS m/z: found for $[M]^+$ 1141.67 (calcd. for $[M]^+$ m/z 1141.40). UV-Vis (THF): λ_{max}, nm (log ε): 333 (5.0), 682 (5.2). Calcd for $C_{76}H_{56}CoN_8$: C 80.05, H 4.95, N 9.83 %; found C 80.02, H 4.91, N 9.78.

2.3.3 Synthesis of Phthalocyanine 2 b,c

The appropriate tetraiodo-phthalocyanine (**1b,c** for **2b,c**) (0.090 mmol) was reacted with 0.130 g of 1-ethynyl-2,4,5-trimethylbenzene (0.90 mmol) and as the catalyst of homogeneous C–C coupling, $[(Ph_3P)_2PdCl_2]$ (1 μmol) was used, and copper(I) iodide (0.5 μmol) was the co-catalyst in this reaction. A solvent mixture of triethylamine (freshly distilled, 4 mL) and tetrahydrofuran (2 mL) was employed. Under nitrogen atmosphere, the contents were stirred at room temperature for 24 hours. The dark green reaction mixture was cooled and a precipitation mixture of methanol:water (3:1 V:V) mixture was added until a sign of precipitation was observed. The formed precipitate was filtered and washed several times with ethanol and methanol as a first purification step. The green-colored product was charged onto silica gel (stationary phase) and methanol:tetrahydrofuran (30:1 V:V) and then n-hexane:1,4-dioxane (5:2 by volume) were used as the mobile phases. Finally, the product was centrifuged in hot acetone and this process is repeated until it is pure.

2.3.3.1 2,9 (10), 16 (17), 23 (24)-Tetrakis [(2,4,5-trimethylphenyl)ethynyl] Phthalocyaninatozinc (II) (2 b)

Yield: 0.0288 g (28 %). mp >300 °C. IR (ν, cm^{-1}): 3012–2964 (C–H, aromatic), 2912–2861 (C–H aliphatic), 2200 (C≡C). ^{1}H NMR (500 MHz; (DMSO-d_6): δ H, ppm 8.88–8.70 (m, 8H, Ar–H), 8.11–8.04 (m, 4H, Ar–H), 7.56–7.52 (m, 4H, Ar–H), 7.20 (s, 4H, Ar–H), 2.70 (s, 12H, CH_3), 2.32 (s, 24H, CH_3) UV-Vis (THF): λ_{max}, nm (log ε): 369 (5.1), 695 (5.6). MALDI-TOF-MS m/z: found for $[M+2H]^+$ 1146.08 (calcd. for $[M]^+$ m/z 1144.39). Calcd for $C_{76}H_{56}N_8Zn$: C 79.60, H 4.92, N 9.77 %; found C 79.51, H 4.87, N 9.72,

2.3.3.2 2,9 (10), 16 (17), 23 (24)-Tetrakis [(2,4,5-trimethylphenyl)ethynyl]phthalocyanina-tochloromanganese(III) (2 c)

Yield : 0.0326 g (31 %). mp >300 °C. IR (ν, cm^{-1}): 3057 (C–H, aromatic), 2915–2857 (C–H aliphatic), 2198 (C≡C). UV-Vis (THF): λ_{max}, nm (log ε): 358 (4.7), 739 (5.05). MALDI-TOF MS m/z: found for $[M–H–Cl]^+$ 1135.24 (calcd. for $[M]^+$ 1171.70). Calcd for $C_{76}H_{56}ClMnN_8$: C 77.90, H 4.82, N 9.56 %; found C 77.83, H 4.89, N 9.52.

3 Results and Discussion

3.1 Synthesis and Characterization

The synthesis of the phthalonitrile derivative was carried through the Sonogashira cross-coupling reaction. Pd catalyzed alkylation, the coupling reaction of terminal alkynes with aryl or vinyl halides, is a method used frequently in recent years. The reaction takes place in a basic medium with aliphatic or cycloaliphatic amine-type solvent, catalyzed by palladium complex and copper (I) halide. The synthesis of the new phthalonitrile derivative was first performed under typical Sonogashira reaction conditions. 4-Iodophthalonitrile and 1-ethynyl-2,4,5-trimethylbenzene were cross-coupled in trimethylamine/THF solvent mixture to give 4-[(2,4,5-trimethylphenyl)ethynyl]phthalonitrile (**2**). The reaction proceeded with $[(Ph_3P)_2PdCl_2]$ and CuI as catalyst and co-catalyst, respectively, at 50 °C under nitrogen atmosphere with 71 % yield. The crude product was purified by column chromatography using silica gel in CH_2Cl_2: n-hexane mixture. The novel phthalonitrile compound was characterized by FT-IR and ^{1}H and ^{13}C-NMR. FT-IR spectrum of **2** indicated that the compound has C≡N (2228 cm^{-1}), C≡C (2210 cm^{-1}), and aromatic groups (3067 cm^{-1}), respectively. In the ^{1}H-NMR($CDCl_3$) spectrum of compound **2**, aromatic protons were in the range of 7.89–7.05 ppm, and aliphatic protons were in the range of 2.44–2.25 ppm. In the ^{13}C-NMR($CDCl_3$) spectrum, especially the carbons of the nitrile and C≡C group were observed at 116.24, 115.28 (C≡N) and 96.57, 88.95(C≡C) ppm. These characterization results show that phthalonitrile **2** was successfully synthesized.

The synthesis of novel compounds (**2,2a–c**) is shown in Scheme 1. General methods were employed to perform template cyclotetramerization on the phthalonitrile to form metallophthalocyanines in the presence of appropriate metal salts in different basic solvents. Except for cobalt phthalocyanine, yields were found to be quite low even if the reaction conditions (solvent, temperature, time, etc.) were changed. Considering these results, the second alternative synthesis method was applied. Metal

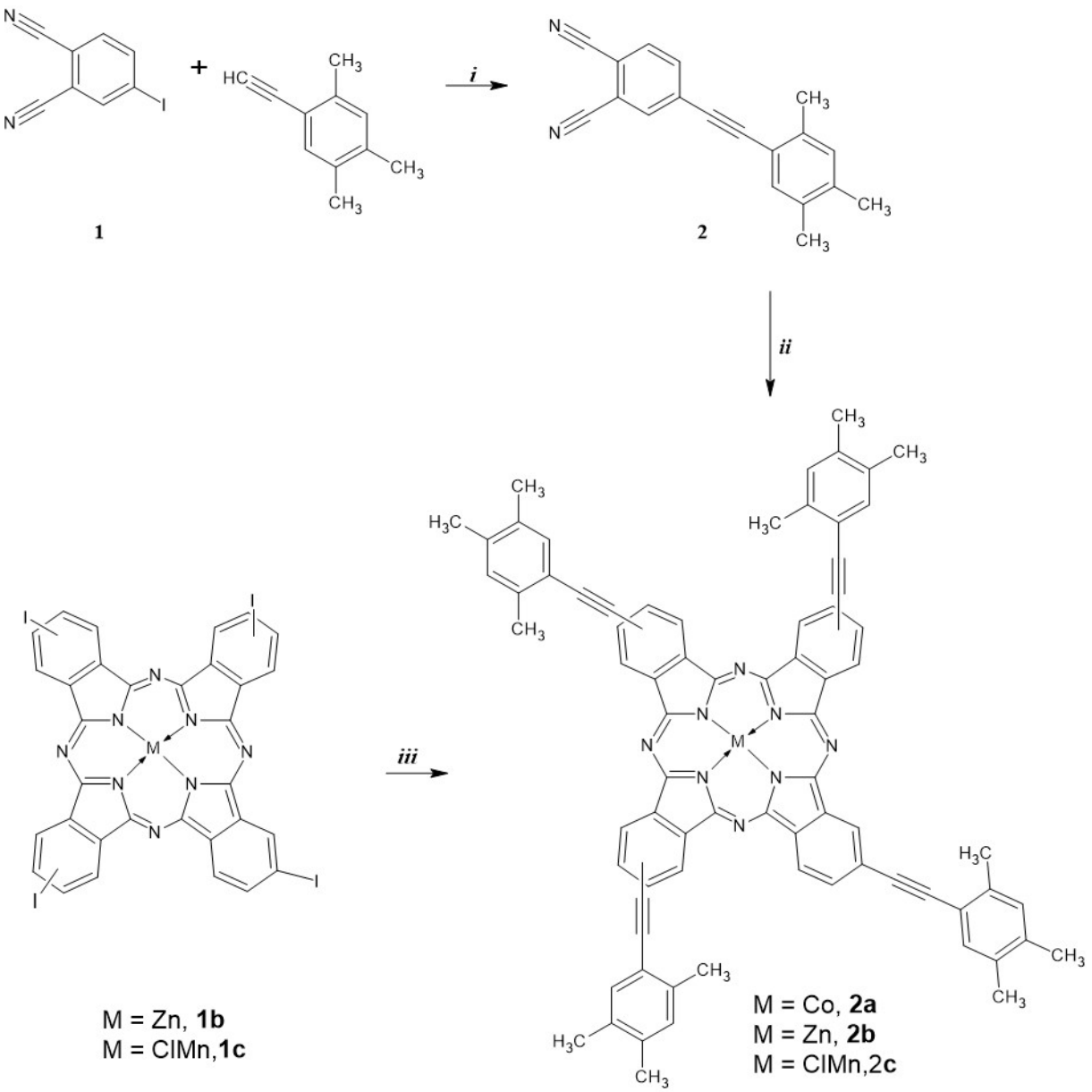

Scheme 1. Synthesis of the metallophthalocyanine compounds **2a–c**. **i**: THF/ NEt_3, CuI, $[Pd(PPh_3)_2Cl_2]$, 50 °C, 24 h. **ii**: $CoCl_2$, N,N-dimethylaminoethanol, 145 °C, 24 h, **iii**: THF/ NEt_3, CuI, $[Pd(PPh_3)_2Cl_2]$, 50 °C, 24 h.

derivatives of alkynyl-containing phthalocyanines can also be prepared by Sonogashira cross-coupling reactions between phthalonitrile derivatives and tetraiodo-substituted metallophthalocyanines. The synthesis of the intended metal phthalocyanines was carried out by this second approach. The tetraiodo metallophthalocyanines [ZnPc and ClMnPc] **1b–c** were synthesized as mentioned elsewhere [35].

As a continuation of our reaction scheme, compounds **1b–c** were reacted with 1-ethynyl-2,4,5-trimethylbenzene in the presence of bis[triphenylphosphine]palladium(II) chloride ($[Pd(PPh_3)_2Cl_2]$) and copper(I) iodide as catalytic entities in THF /triethylamine (1:2) solvent mixture to yield phthalocyanines **2b–c** in 28 % and 31 % yields, respectively. They were characterized by using standard spectral methods (FT-IR, ^{1}H NMR, UV-Vis and mass spectra) As shown in the experimental section, the proposed structures are in good agreement with the spectral data. The FT-IR spectra of Pcs **2a–c** exhibit typical vibrations corresponding to the substituent groups (aromatic, aliphatic C–H and C≡C groups) around similar frequencies. Especially, the stretching vibrations belonging to the C≡C groups of Pcs **2a–c** were clearly observed at 2203 cm^{-1}, 2200 cm^{-1} and 2198 cm^{-1}, respectively. m/z = 1141.67 $[M+H]^+$ for **2a** (CoPc) helps conform to the proposed structure. However, due to paramagnetic nature of cobalt (II) ion, no ^{1}H NMR measurements for **2a** could be measured. ^{1}H NMR spectrum of ZnPc (**2b**) compound

in DMSO-d_6 shows that the 24 aromatic protons (phthalocyanine and substituent rings) resonated between 9.03 and 7.52 ppm while 36 aliphatic protons of substituents resonated between 2.70 and 2.32 ppm. The $[M–Cl]^+$ molecular ion peak was observed at m/z = 1135.24 for ClMnPc(III) **(2c)** and confirmed the structure of the compound.

Metallophthalocyanines are characterized by two strong bands in the UV-Vis spectrum. The first of these is the Soret (B) band, between 300–400 nm, and the other is the Q band between 650–700 nm and both bands arise from different levels of π-π* transitions [39-42]. The UV spectra of the complexes were recorded in THF as solvent, and for all complexes, intense Q band absorptions at 682, 695 and 739 nm for compounds **2a–c**, respectively, and the B band also recorded between 333–369 nm. In order to investigate the aggregation properties, the UV-Vis spectra of the compounds in the range of 2–14 × 10^{-6} M in THF were examined and compliance with the Lambert-Beer law was demonstrated at these concentration ranges. That is, it explains that the studied phthalocyanines are monomeric. In addition, Q bands in UV-Vis spectra of all phthalocyanine compounds taken in different solvents (DMF, DMSO, chloroform, toluene, and THF) at 6×10^{-6} M concentration were observed as expected.

3.2 Voltammetry of the Compounds

In the electrochemical measurements, we used glassy carbon electrode (GCE) in dimethylsulfoxide (DMSO)/tetrabutylammonium perchlorate (BAP) medium. Then, as seen in Table 1, half wave potentials ($E_{1/2}$) values were derived from the analyses of the recorded voltammograms. According to the table, $E_{1/2}$ values of the complexes are in harmony with the similar MPcs reported in the literature. Due to the different substituent environments, slight potential shifts for the couples are observed in addition to the changing on the reversibility of the redox processes.

CVs and SWVs of CoPc (2a) and ZnPc (2b) were given in the Figure SM1-2 for comparative purposes. Here, detailed analysis of MnPc (2c) is discussed as an example. Figure 1 represents CVs and SWVs of MnPc (2c). MnPc has Cl^{1-}-Mn^{III} metal center which is redox active when it is incorporated in the Pc core. Thus, as shown in Figure 1, two metal based reduction processes, $[Cl^{1-}\text{-}Mn^{III}Pc^{2-}]/[Cl^{1-}\text{-}Mn^{II}Pc^{2-}]^{1-}$ and $[Cl^{1-}\text{-}Mn^{II}Pc^{2-}]^{1-}/[Cl^{1-}\text{-}Mn^{I}Pc^{2-}]^{2-}$, are observed at 0.01 V (Red(1)) −0.66 V (Red(2)) respectively in addition to the Pc reduction processes at −1.19 V (Red(3)) and −1.65 V (Red(4)). Figures 1a and b show that all reduction processes appear as chemically and electrochemically reversible and ΔE_p and I_{pa}/I_{pc} values of the redox couples support reversibility of the processes. However, SWVs of the complex indicate that there were chemical reactions after redox reactions. The small waves at −1.39 and −1.80 V in Figure 1c probably result from the chemical reaction products. The chemical reaction may be the release of the axial Cl_1- ligand after the metal based reduction processes. It is well reported in the literature that when the oxidation state of a ligand decreases, its coordination number also decrease [43]. Thus after the first reduction reaction, $[Cl^{1-}\text{-}Mn^{II}Pc^{2-}]^{1-}$ species release the Cl^{1-} ion and form $[Mn^{II}Pc^{2-}]$ species which give its reduction processes at −1.39 and −1.80 V. These enhanced redox activities, metal based characters, and reversibility of the process increases the value of the for the various electrochemical technologies. As shown in Table 1, and as reported in the literature, Redox responses of the Pcs are considerably influenced the electrochemical character of the complexes. The electron transfer processes of the complexes studied here generally shifts towards the positive potentials due to the extending of the π electron conjugation. This is the one of the rare studies for the recording of at least three Pc based reduction with ZnPc and a metal

Table 1. Electrochemical data of the complexes in the DMSO/TBAP electrolyte system. All potential values are calculated versus Ag/AgCl.

Complexes	$E_{1/2}$ (V) of Redox Processes Red(1)	Red(2)	Red(3)	Red(4)	Oxd(1)	Oxd(2)	Ref.
CoPc (2a)	−0.23	−1.16	−1.67		0.42	1.34	tw
ZnPc (2b)	−0.68	−0.90 (−1.20)	−1.66		0.82	–	tw
ClMnPc (2c)	0.01	−0.66	−1.19	−1.65	–	–	tw
CoPc	−0.48	−1.29	−1.92		0.30	0.91	[44a]
CoPc(t-SA)	−0.62	−0.95	−1.63		0.67	0.89	[47]
CoTMPyrPc	−0.50	−1.34	−1.93		0.47	1.00	[48]
CoPc	−0.38	−1.45			0.77	1.07	[31c]
ZnPc-CB1	−1.03	−1.35			1.01		[49]
ZnPc-CB2	−1.05	−1.38			1.03		[49]
ZnPc	−0.82	−1.41			0.63		[50]
ClMnPc	−0.30	−0.90	−1.36		0.38 (0.51)	0.88	[44]
			−1.88				
MnTMPyrPc	−0.06	−0.68	−1.19		–	–	[48]
ClMnPc(m)	−0.23	−0.80	−1.04		–	–	[51]
MnPc	−0.26	−0.65	−1.26		0.59	1.03	[52]
MnPc	−0.30	−1.02			1.06	1.03	[53]

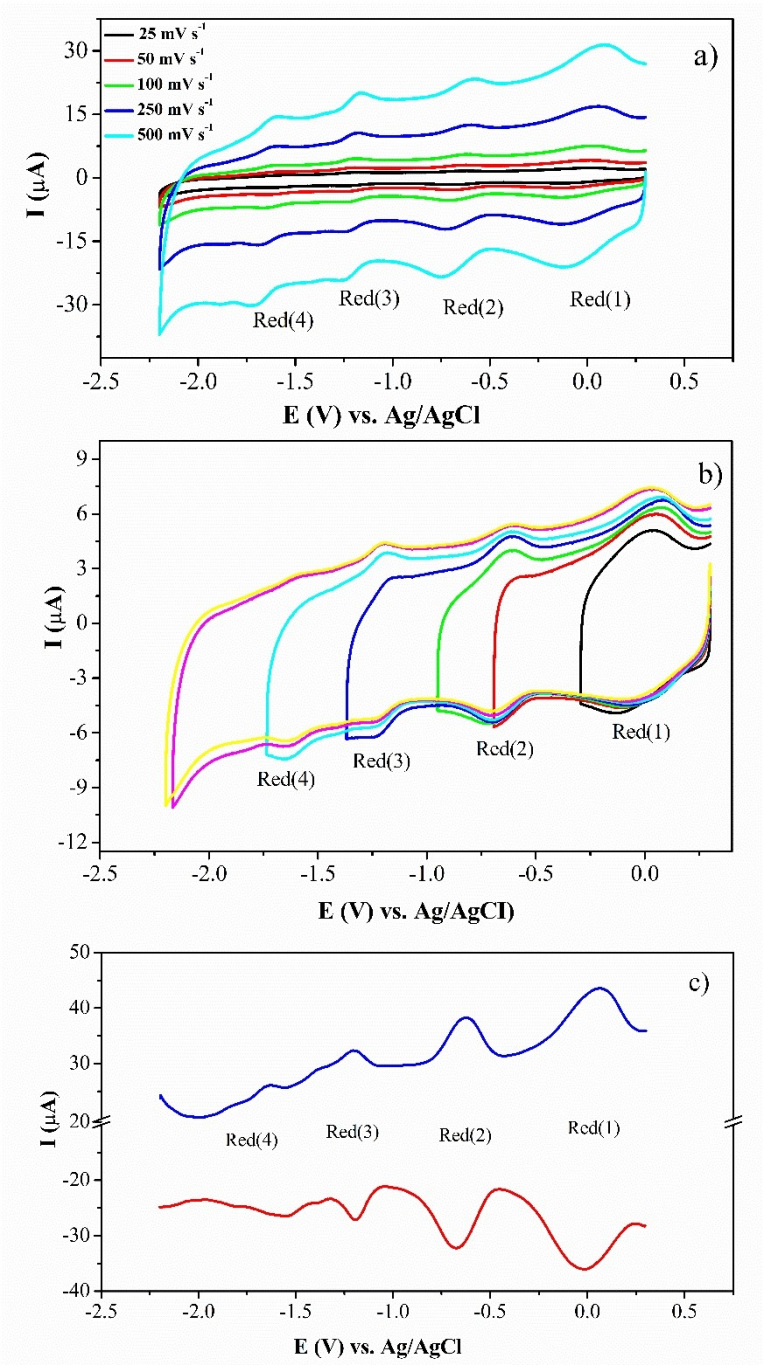

Fig. 1. At various scan rates, voltammograms of MnPc (5.0×10^{-4} mol.dm^{-3}) were recorded on a GCE working electrode in DMSO/TBAP a) CVs b) CVs recorded with different switching potentials and c) SWVs.

based, and two Pc based reduction with CoPc. Similarly, two metal based and two Pc based reduction processes could be observed due to the shifting of the reduction processes towards the zero potential, which is resulted with the influence of the extension of the π electron conjugation with trimethylphenylethynyl moieties.

3.3 In-situ Spectroelectrochemistry

In-situ spectroelectrochemistry (SEC) and spectrocolorimetry (SC) were employed so as to support the redox mechanisms proposed by voltammetric analyses and they illustrated color changes during redox processes. As shown in Figure 2, characteristic spectral changes are recorded for the Pc based redox processes. For ZnPc, the intensity of the Q band changes, and new bands are

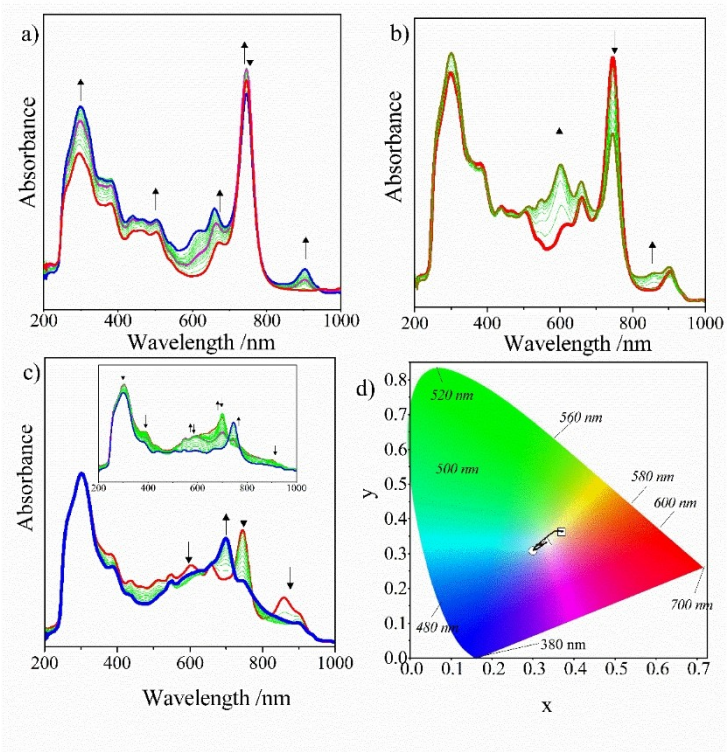

Fig. 2. In-situ UV-Vis spectral changes of ZnPc in DMSO/TBAP a) $E_{app} = -0.75$ V b) $E_{app} = -1.40$ V, c) $E_{app} = 1.00$ V, d) Each symbol shows the electro-generated species in the chromaticity diagram. □: $[Zn^{II}Pc^{-2}]$; Δ:$[Zn^{II}Pc^{-3}]^{1-}$; O: $[Zn^{II}Pc^{-4}]^{2-}$; ☆: $[Zn^{II}Pc^{-1}]^{1+}$.

observed in the LMCT (ligand to metal charge transfer) region, therefore the redox couples are assigned to ligand-based electron transfer. Figure 2d shows the chromaticity diagram obtained with SC measurements, and distinct color changes were recorded during redox reactions. These responses indicate possible function of ZnPc as electro-chromophoric material.

Spectroelectrochemical responses of CoPc was given in Figure SM3. Its spectral changes are in harmony with similar CoPc compounds in the literature and they support the redox mechanism suggested by voltammetric analyses [44]. The spectral changes of MnPc is completely different than those of CoPc and ZnPc owing to two metal-based reductions and chemical reactions as shown in Figure 3. In the first reduction reaction, the Q band at 745 nm decreases in intensity while the band at 661 nm increases. In addition, a new band at 903 nm is formed (Figure 3a). Especially the bands at 661 and 903 nm show the formation of $[Cl^{1-}\text{-}Mn^{II}Pc^{2-}]^{1-}$ species because of the reduction of $[Cl^{1-}\text{-}Mn^{III}Pc^{2-}]$ at −0.30 V constant applied potential [43b, 45]. Figure 3b represents spectral changes observed in the second reduction reaction. New bands at 600 and 856 nm indicate the reduction of $[Cl^{1-}\text{-}Mn^{II}Pc^{2-}]^{1-}$ to $[Cl^{1-}\text{-}Mn^{I}Pc^{2-}]^{2-}$ species. The spectral changes observed in the processes of Red(3) and Red(4) depict further Pc-based reductions of $[Cl^{1-}\text{-}Mn^{I}Pc^{2-}]^{2-}$ species (Figure 3c) [43b,45,46]. Observation of different trends for the spectral changes shown in Figure 3c inset indicates chemical irreversibility of the fourth reduction process due to the preceding chemical reactions. Continuous changes of the trends like ZnPc and CoPc, sharp color changes are also observed with the ClMnPc as shown in the chromaticity diagram in Figure 3d. The initial orange species (x = 0.370 and y = 0.364), pertaining to the neutral $[Cl^{1-}\text{-}Mn^{III}Pc^{2-}]$ changes to green (x = 0.340 and y = 0.357) and blue (x = 0.296 and y = 0.308) at the end of the first and second reduction processes respectively, and then it changes to colorless (x = 0.335 and y = 0.332) at the end of the third reduction process. Due to these rich redox responses and various color displays, MnPc can be used as electrochromic material.

3.4 Electrochromism of ITO/MPc/Nf Electrodes

All complexes are coated on ITO substrate and ITO/MPc/Nf electrodes are prepared for their possible usage as electrochromic materials. ITO/ZnPc/Nf electrodes were characterized with SEM and FT-IR techniques. As shown in Figure SM4, a homogeneous ZnPc/Nf film was seen on the ITO surface. A smooth and a dense characteristic on the film is seen and no obvious phase separation phenomena was observed. The average film thicknesses were determined from the cross-sectional SEM images as 481, 438, and 437 nm for ITO/ZnPc/Nf, ITO/MnPc/Nf, and ITO/CoPc/Nf respectively (Figure SM5). The chemical structure of ZnPc/Nf film on the ITO surface is described with FT-IR spectra, as represented in Figure SM6, the characteristic absorption bands of ZnPc are

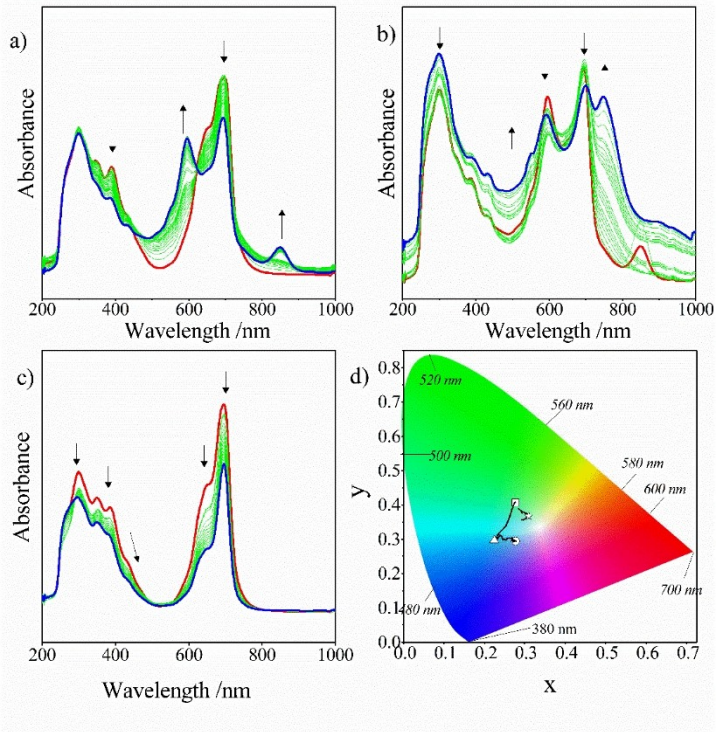

Fig. 3. In-situ UV-Vis spectral changes of MnPc in DMSO/TBAP electrolyte system a) Eapp = −0.30 V b) Eapp = −0.80 V, c) Eapp = −1.30 V and then −1.90 V, d) Chromaticity diagram (Symbols shown as □, O, Δ,* denote the color of the electrogenerated species.); □: [Cl^{1-}-$Mn^{III}Pc^{-2}$]; O :[Cl^{1-}-$Mn^{II}Pc^{-2}$]$^{1-}$; Δ: [Cl^{1-}-$Mn^{I}Pc^{-2}$]$^{2-}$; *: [Cl^{1-}-$Mn^{I}Pc^{-3}$]$^{3-}$.

observed at 3066 cm $^{-1}$ (aromatic C–H stretch), 2922 cm^{-1} and 2852 cm^{-1} (aliphatic C–H stretch) and 1608 cm^{-1} (N–H bend). The absorption peaks determined at 740–1690 cm^{-1} ascribable to the characteristic absorptions of Pc cores except the C–O-C stretching band of Nafion at 875 cm^{-1}. UV-Vis spectral changes of ITO/MPc/Nf electrodes are recorded under 1.30 V applied potential. As shown in Figure 4, pronounced spectral changes are observed in the visible region of the light spectrum, which cause distinct color changes on the ITO/MPc/Nf electrodes in AN/TBAP electrolyte. Thus, all electrochromic responses of these electrodes are tested, and derived parameters are listed on Table 2. As shown in this table, altering the metal center of MPcs influence the color changes, response time and optical contrast parameters of the electrodes. Detailed electrochromic results of ITO/ZnPc/Nf electrode is represented in Figure 5 as an example for ITO/MPc/Nf electrodes. Repetitive chronoamperometric (rCA) excitations are applied to the ITO/ZnPc/Nf electrode with 30 s time intervals in the range of 0.0 V and 1.30 V to test the electrochromic responses of the electrode, and T% responses and color changes are recorded according to rCA excitations. As can be seen from Figure 5a, the results of the stable cathodic and anodic currents observed during the rCA show the coulombic stability of the electrode. Because of the oxidation of the ZnPc film on the ITO/ZnPc/Nf electrode, fast and almost stable and fast T% changes are observed with each rCA cycle. Whereas the %T responses increased slightly when rCA excitations were 1.30 and 0.00 V, optical contrast in each cycle remains almost constant during 25 rCA cycles. Responses times for each color changes are derived from the T% responses vs time, which are recorded as 1.2 s and 1.6 s under 1.30 and 0.0 V potential applications respectively. The color of the green ITO/ZnPc/Nf electrode (point □ x = 0.316 and y = 0.410) turns to red (point □ x = 0.392 and y = 0.335) when 1.30 V potential is applied as shown in Figure 5c. The color of the green electrode changes to red. When these electrochromic parameters are compared with those of the similar studies in the literature, ITO/MPc/Nf electrodes illustrate reasonable electrochemical responses for their possible usages.

4 Conclusion

In the first stage of the synthesis part of this study, the synthesis of new phthalonitrile containing (2,4,5-trimethylphenyl)ethynyl moieties, and in the second stage, the synthesis of tetrasubstituted metal (cobalt, zinc and chloromanganese) phthalocyanines containing the same ethynyl moieties in the peripheral position was carried out by choosing the most appropriate procedure to obtain the highest yield. The characterization, aggregation properties, electrochemical and spectroelectrochemical measurements of these new metalophthalocyanines were inves-

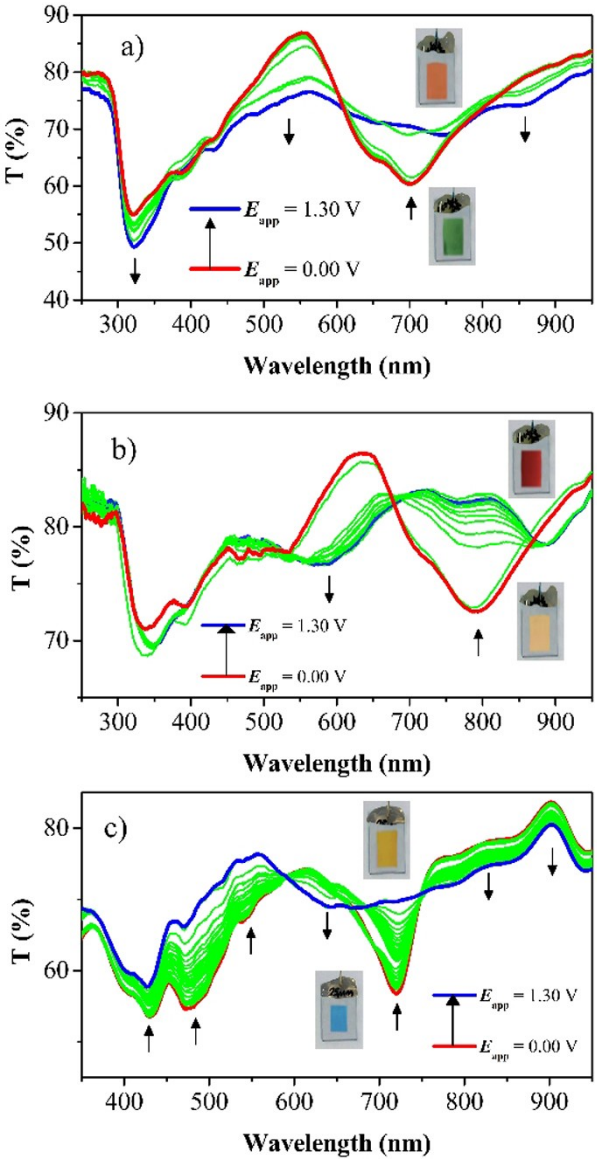

Fig. 4. In situ spectroelectrochemical (T% vs. wavelength) responses of the electrodes under E_{app} 1.30 V (30 s) in AN/TBATFB electrolyte. a) ITO/ZnPc/Nf; b) ITO/MnPc/Nf; c) ITO/CoPc/Nf.

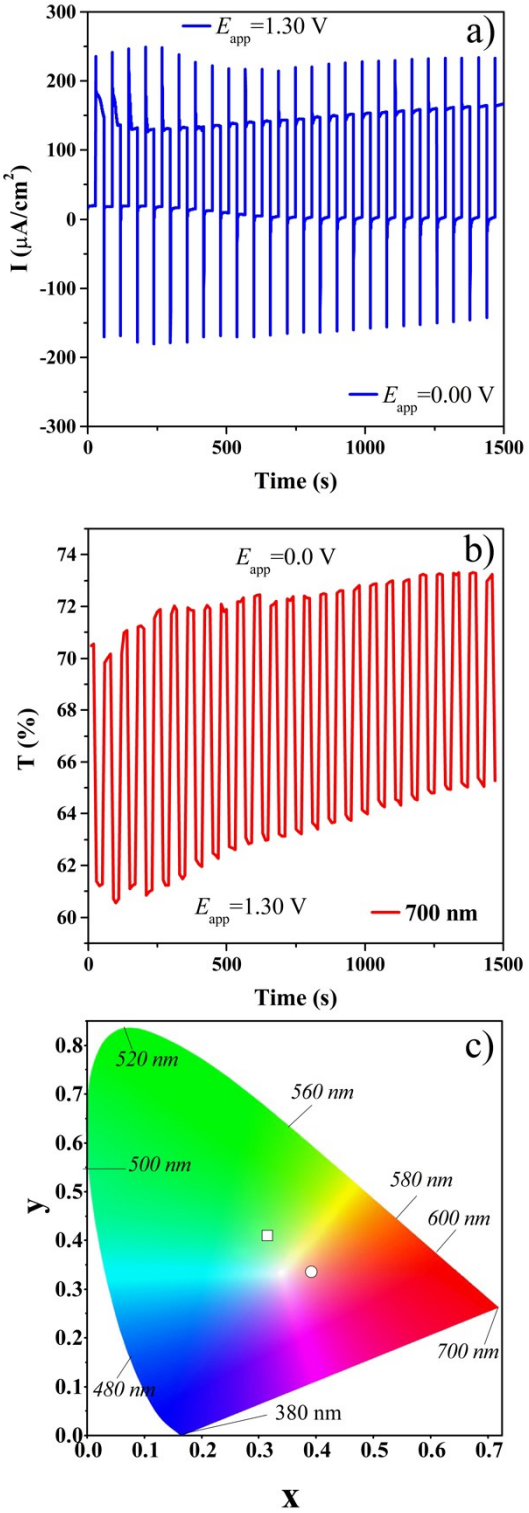

Fig. 5. Electrochromism of ITO/ZnPc/Nf electrode. a) Repetitive chronoamperometry (rCA), b) %T (versus time (30s)) in 700 nm, responses between E_{app} = 0.00 V–1.30 V in AN/TBATFB electrolyte, c) chromaticity diagram.

tigated. Redox responses of MPcs indicates that incorporating different metal to the center of MPc considerably altered the electrochemical mechanism of the complexes. While ZnPc illustrate only Pc based electron transfer reactions, Co^{II} and $ClMn^{III}$ metal centers gave extra redox processes. Generally, all complexes gave multi-electron redox couples which increase their value for the electrochemical applications. Color changes observed during in situ spectroelectrochemical measurements showed their electrochromic functionality, thus MPc based electrodes were prepared and tested as electrochromic electrodes. In situ SCC responses of ITO/MPc/Nf electrodes represented reasonable electrochromic responses with fast and stable color changes. In particular, it has been shown that MnPc can be used as an electrochromic material due to its rich redox reaction and various color responses.

Table 2. Electrochromic parameters of metal phthalocyanine materials.

Complexes	Electrolyte system	$E_{app.}$ (V)	% T[a]	Response time (s)[b]	Color	[c] CIE 1931 xyz chromaticity coordinates	Current stability loss[d]	%T stability loss[e]	Optical contrast[f]	Ref.
ITO/ZnPc/Nf (at 700 nm)	AN/ TBATFB	*0.0*	60	1.60	green	x = 0.316; y = 0.410	2.1	3.5	11	tw
		1.30	71	1.20	red	x = 0.392; y = 0.335	11.2	6.5		
ITO/MnPc/Nf (at 785 nm)	AN/ TBATFB	*0.0*	72	3.2	orange	x = 0.372; y = 0.376	3.0	2.2	10	tw
		1.30	82	4.5	red	x = 0.374; y = 0.346	3.2	2.7		
ITO/CoPc/Nf (at 720 nm)	AN/ TBATFB	*0.0*	56	1.60	cyan	x = 0.286; y = 0.346	4.3	3.7	13	tw
		1.30	69	1.20	orange	x = 0.367; y = 0.346	3.7	5.2		
ITO/PANI-N_3-TA-MnPc (at 500 nm)	$LiClO_4/H_2O$	*0.0*	72	0.55	green	x = 0.244; y = 0.368	0.0 (9.0)	0.0 (5.2)	20	[54]
		1.20	52	0.50	brown	x = 0.338; y = 0.250	0.0 (7.2)	0.0 (11.5)		
ITO/NiPc-tdea	AN/TBAP	*0.0*	59	1.8	cyan	x = 0.316; y = 0.336	–	–	20	[55]
		1.20	79	1.0	red	x = 0.418; y = 0.337	–	–		
ITO/H_2Pc-tdea	AN/TBAP	*0.0*	59	8.0	cyan	x = 0.299; y = 0.331	–	–	40	[55]
		1.20	99	5.0	light yellow	x = 0.358; y = 0.351	–	–		
H_2Pc-THQD	AN/TBAP	*0.0*	65	2.0	green	x = 0.313; y = 0.360	18.5	10	45	[56]
		1.20	90	3.0	blue	x = 0.324; y = 0.254	19	6		
ITO/NiPc-THQD	AN/TBAP	*0.0*	18	2.5	green	x = 0.270; y = 0.431	10.8	4	62	[56]
		1.20	80	2.5	blue	x = 0.293; y = 0.246	10.7	1		

Acknowledgements

This work was supported by TUBITAK (Project no: 118Z731) and the Research Fund of the Technical University of Istanbul (Project no: TYL-2020-42662). Atıf Koca would like to thank the Turkish Academy of Sciences (TUBA) for their support.

Data Availability Statement

The data that support the findings of this study are available from the corresponding author upon reasonable request.

References

[1] M. B. Nielsen, F. Diederich, *Chem. Rev.* **2005**, *105(5)*, 1837–1868.
[2] G. Bottari, D. D. Díaz, T. Torres, *J. Porphyrins Phthalocyanines* **2006**, *10(9)*, 1083–1100.
[3] S. Toyota, *Chem. Rev.* **2010**, *110(9)*, 5398–5424.
[4] P. Şen, F. Dumludağ, B. Salih, A. R. Özkaya, Ö. Bekaroğlu, *Synth. Met.* **2011**, *161(13–14)*, 1245–1254.
[5] G. Hughes, M. R. Bryce, *J. Mater. Chem.* **2005**, *15(1)*, 94.
[6] D. Gounden, N. Nombona, W. E. Van Zyl, *Coord. Chem. Rev.* **2020**, *420*, 213359.
[7] R. Zhou, F. Josse, W. Gopel, Z. Z. Ozturk, O. Bekaroglu, *Appl. Organomet. Chem.* **1996**, *10(8)*, 557–577.
[8] X. Li, S. Lee, J. Yoon, *Chem. Soc. Rev.* **2018**, *47(4)*, 1174–1188.
[9] N. Brasseur, R. Ouellet, C. La Madeleine, J. E. van Lier, *Br. J. Cancer* **1999**, *80(10)*, 1533–1541.
[10] M. Soncin, A Busetti, R. Biolo, G. Jori, G. Kwag, Y. S. Li, M. E. Kenney, M. A. J. Rodgers, *J. Photochem. Photobiol. B* **1998**, *42(3)*, 202–210.
[11] V. Cakir, M. Goksel, M. Durmus, Z. Biyiklioglu, *Dyes Pigm.* **2016**, *125*, 414–425.
[12] C. Uslan, B. Ş. Sesalan, *Inorg. Chim. Acta* **2013**, *394*, 353–362.
[13] H. P. Karaoglu, O. Saglam, S. Ozdemir, S. Goncac, M. B. Kocak, *Dalton Trans.* **2021**, *50*, 9700–9708.
[14] R. Olgac, T. Soganci, Y. Baygu, Y. Gök, M. Ak, *Biosens. Bioelectron.* **2017**, *98*, 202–209.
[15] P. Talvenmaa, *Intelligent Textiles and Clothing* **2006**, 193–205. ISBN 978-1-84569-005-2, Woodhead Publishing
[16] O. Sato, *J. Solid State Electrochem.* **2007**, *11(6)*, 773–779.
[17] P. S. Patil, R. K. Kawar, S. B. Sadale, *Electrochim. Acta* **2005**, *50(12)*, 2527–2532.

[18] E. Avendaño, A. Azens, G. A. Niklasson, C. G. Granqvist, *Sol. Energy Mater. Sol. Cells* **2004**, *84(1–4)*, 337–350.
[19] P. M. S. Monk, R. D. Fairweather, M. D. Ingram, J. A. Duffy, *J. Electroanal. Chem.* **1993**, *359(1–2)*, 301–306.
[20] R. J. Mortimer, A. L. Dyer, J. R. Reynolds, *Displays* **2006**, *27(1)*, 2–18.
[21] M. L. Rodriguez-Méndez, M. Gay, J. A. de Saja, *J. Porphyrins Phthalocyanines* **2009**, *13(11)*, 1159–1167.
[22] S. H. Jung, C.-S. Ha, *High Perform. Polym.* **2006**, *18(5)*, 679–696.
[23] A. Gupta, J. H. Lee, J. H. Seo, S. G. Lee, J. S. Park, *RSC Adv.* **2015**, *5(90)*, 73989–73992.
[24] İ. Özçeşmeci, A. K. Burat, Z. A. Bayır, *J. Organomet. Chem.* **2014**, *750*, 125–131.
[25] E. Kumral, H. Y. Yenilmez, S. Albayrak, A. N. Şahin, A. Altındal, Z. A. Bayır, *Dalton Trans.* **2020**, *49*, 9385–9392.
[26] E. Fourie, J. C. Swarts, I. Chambrier, M. J. Cook, *Dalton Trans.* **2009**, *7*, 1145–1154.
[27] T. Furuyama, K. Satoh, T. Kushiya, N. Kobayashi, *J. Am. Chem. Soc.* **2014**, *136(2)*, 765–776.
[28] H. Y. Yenilmez, A. N. Şahin, A. Altındal, Z. A. Bayır, *Synth. Met.* **2021**, *273*, 116690.
[29] C. Farley, N. V. S. D. K. Bhupathiraju, B. K. John, C. M. Drain, *J. Phys. Chem. A* **2016**, *120(38)*, 7451–7464.
[30] a) I. A. Akinbulu, *Polyhedron* **2010**, *29*, 1257–1270; b) R. Li, X. Zhang, P. Zhu, D. K. Ng, N. Kobayashi, J. Jiang, *Inorg. Chem.* **2006**, *45*, 2327–2334.
[31] a) F. Demir, H. Y. Yenilmez, A. Koca, Z. A. Bayır, *J. Electroanal. Chem.* **2019**, *832*, 254–265; b) Y. Gök, H. Z. Gök, M. K. Yılmaz, M. Farsak, İ. Ü. Karayiğit, *Polyhedron* **2018**, *153*, 128–138; c) E. T. Acar, T. A. Tabakoglu, D. Atilla, F. Yuksel, G. Atun, *Polyhedron* **2018**, *152*, 114–124.
[32] A. M. Sevim, H. Y. Yenilmez, M. Aydemir, A. Koca, Z. A. Bayır, *Electrochim. Acta* **2014**, *137*, 602.
[33] S. M. Mareuccio, P. I. Svirskaya, S. Greenberg, A. B. P. Lever, C. C. Leznoff, *Can. J. Chem.* **1985**, *63*, 3057.
[34] A. M. Sevim, H. Y. Yenilmez, Z. A. Bayır, *Polyhedron* **2013**, *62*, 120.
[35] E. M. Maya, P. Haisch, P. Vázquez, T. Torres, *Tetrahedron* **1998**, *54*, 4397.
[36] A. Koca, M. Ozcesmeci, E. Hamuryudan, *Electroanalysis* **2010**, *22(14)*, 1623–1633.
[37] R. Z. U. Kobak, D. Akyüz, A. Koca, *J. Solid State Electrochem.* **2016**, *20(5)*, 1311–1321.
[38] F. Demir, H. Y. Yenilmez, A. Koca, Z. A. Bayır, *J. Electroanal. Chem.* **2019**, *832*, 254–265.
[39] N. Farajzadeh, Ç. Çelik, G. Y. Atmaca, S. Özdemir, S. Gonca, A. Erdoğmuş, M. B. Koçak, *Dalton Trans.* **2021**, DOI: 10.1039/d1dt02919c.
[40] S. Tuncer, K. Kaya, I. Ozcesmeci, A. K. Burat, *J. Organomet. Chem.* **2017**, *827*, 78–85.
[41] Z. A. Bayır, *Dyes Pigm.* **2005**, *65(3)*, 235–242.
[42] A. Kalkan, A. Koca, Z. A. Bayır, *Polyhedron* **2004**, *23(18)*, 3155–3162.
[43] a) K. I. Ozoemena, T. Nyokong, *Electrochim. Acta* **2006**, *51*, 2669–2677; b) İ. Özçeşmeci, A. Koca, A. Gül, *Electrochim. Acta* **2011**, *56*, 5102–5114; c) D. Arıcan, M. Arıcı, A. L. Uğur, A. Erdoğmuş, A. Koca, *Electrochim. Acta* **2013**, *106*, 541–555.
[44] a) D. Akyüz, T. Keleş, Z. Biyiklioglu, A. Koca, *J. Electroanal. Chem.* **2017**, *804*, 53–63; b) Ü. Demirbaş, D. Akyüz, H. T. Akçay, A. Koca, E. Menteşe, H. Kantekin, *J. Mol. Struct.* **2018**, *1173*, 205–212; c) Ö. Kurt, A. Koca, A. Gül, M. B. Koçak, *Synth. Met.* **2015**, *206*, 72–83.
[45] a) A. K. Burat, Z. A. Bayır, A. Koca, *Electroanalysis* **2012**, *24*, 338–348; b) G. Mbambisa, P. Tau, E. Antunes, T. Nyokong, *Polyhedron* **2007**, *26*, 5355–5364; c) T. Nyokong, *Functional Phthalocyanine Molecular Materials* **2010**, 45–87, Springer, Berlin, Heidelberg.
[46] B. Agboola, K. I. Ozoemena, P. Westbroek, T. Nyokong, *Electrochim. Acta* **2007**, *52*, 2520–2526.
[47] K. Sakamoto, E. Ohno, *Dyes Pigm.* **1998**, *37*, 291–306.
[48] J. Obirai, T. Nyokong, *Electrochim. Acta* **2005**, *50*, 3296–3304.
[49] S. Bhattacharya, C. Biswas, S. S. K. Raavi, J. Venkata Suman Krishna, N. Vamsi Krishna, L. Giribabu, V. R. Soma, *J. Phys. Chem. C* **2019**, *123*, 11118–11133.
[50] G. G. Köse, G. K. Karaoğlan, S. N. Işık, D. Akyüz, A. Koca, *Synth. Met.* **2020**, *264*, 116386.
[51] Ü. E. Özen, T. Keleş, Z. Bıyıklıoğlu, A. Koca, A. R. Özkaya, *J. Electrochem. Soc.* **2016**, *163*, B673–B682.
[52] İ. Tağman, M. Özçeşmeci, S. Gümrükçü, İ. Sorar, *J. Mol. Struct.* **2021**, *1245*, 131045.
[53] Y. Ünver, H. Baş, Z. Biyiklioglu, *J. Mol. Struct.* **2019**, *1178*, 508–513.
[54] D. Akyüz, A. Koca, *J. Solid State Electrochem.* **2020**, *24*, 431–440.
[55] F. Demir, Z. Biyiklioglu, A. Koca, *J. Electrochem. Soc.* **2014**, *161*, G1–G6.
[56] D. Arıcan, A. Aktaş, H. Kantekin, A. Koca, *J. Electrochem. Soc.* **2014**, *161*, H670–H676.

Received: March 12, 2022
Accepted: March 29, 2022
Published online on April 12, 2022

